Spectroscopic standards for four- and fivefold-coordinated Fe2+ in oxygen-based minerals

Article *in* American Mineralogist · July 2001

DOI: 10.2138/am-2001-0713

2 authors:

George R Rossman
California Institute of Technology
512 PUBLICATIONS **16,857** CITATIONS

SEE PROFILE

Michail N. Taran
M.P. Semenenko Institute of Geochemistry, Mineralogy and Ore Formation, …
115 PUBLICATIONS **1,003** CITATIONS

SEE PROFILE

American Mineralogist, Volume 86, pages 896–903, 2001

Spectroscopic standards for four- and fivefold-coordinated Fe^{2+} in oxygen-based minerals

GEORGE R. ROSSMAN* AND MICHAEL N. TARAN[1]

Division of Geological and Planetary Sciences, California Institute of Technology, Pasadena, California 91125, U.S.A.

ABSTRACT

Optical spectra are presented for seven oxygen based, four-coordinated Fe^{2+} bearing minerals, eudialyte, gehlenite, genthelvite, gillespite, pellyite, spinel, and staurolite, and two five-coordinated Fe^{2+} minerals, grandidierite and joaquinite. Broad, intense spin-allowed *dd* bands of tetrahedrally coordinated Fe^{2+}, originating from the $^5E \rightarrow {}^5T_2$ transition, appear in the spectral range 3000–7000 cm^{-1}. In the spectra of gillespite and eudialyte, minerals with square-planar coordination, the bands shift to higher energies, appearing in the range 7000–20 000 cm^{-1}. The amount of band splitting depends mainly on the distortion of the ligands surrounding four-coordinated Fe^{2+}. Splitting and distortion are minimal for spinel with a regular tetrahedral site, and maximal for eudialyte and gillespite. For the minerals in four-coordination, the barycenter of the split bands correlates with the sum of the bond-length and edge-length distortion parameters if the square planer sites are excluded from the correlation. Molar absorption coefficients (ε) of the spin-allowed tetrahedral Fe^{2+} bands range from ~20 $cm^{-1}\cdot L\cdot mol^{-1}$ to ~90 $cm^{-1}\cdot L\cdot mol^{-1}$. For eudialyte and gillespite, due to the centrosymmetric character of the ligand environment, the ε values ranges from about 0.5–10 $cm^{-1}\cdot L\cdot mol^{-1}$. For grandidierite and joaquinite, five-coordination causes spectra that resemble those of Fe^{2+} in highly distorted octahedral sites. The number of bands suggests, however, that the electronic level scheme of five-coordinated Fe^{2+} in grandidierite significantly differs from that of Fe^{2+} in octahedral coordination.

INTRODUCTION

Fe^{2+} is one of the most important cations in natural oxide and silicate minerals. Its concentration and distribution within these structures significantly influence the optical, electric, and magnetic properties, including color and pleochroism. Mg-Fe^{2+} intra- and inter-crystalline distributions in natural (Mg, Fe)-bearing silicates are used in modern petrology as a geothermometer and geospeedometer. Site determination of Fe^{2+} is, therefore, one of the main goals of spectroscopic measurements and from this point of view any spectroscopic documentation of Fe^{2+} in various coordinations and symmetries is important.

The optical absorption spectra of Fe^{2+} in octahedral sites of natural crystals have been studied in great detail. This is, however, not the case for Fe^{2+} in tetrahedral coordination, which has been poorly documented in comparison to octahedral Fe^{2+} and needs further investigation. To our knowledge, spectra of only two minerals, spinel (regular MO_4 tetrahedron of T_d symmetry) and staurolite [distorted $MO_2(OH)_2$ tetrahedron], have been presented as examples of electronic *dd* transition of Fe^{2+} ions in tetrahedral sites (e.g., Slack 1964; Dickson and Smith 1976). Also, absorption bands in the spectra of gillespite (Burns et al. 1966) and eudialyte (Pol'shin et al. 1991) have been ascribed to *dd* transitions of Fe^{2+} in a fourfold planar coordination environment.

Investigations of Fe^{2+} in various coordinations, including fourfold ones, are important for interpretation of optical spectra of minerals. Such information may be especially useful when unusual sites of Fe^{2+} such as those of square-planar coordination (Platonov et al. 1979), channel sites (Goldman et al. 1978) or the strongly distorted tetrahedral positions of Be^{2+} (Price et al. 1976; Taran et al. 1989) in the beryl structure are discussed. Note that although the basic crystal field theory of Fe^{2+} in tetrahedral coordination has been worked out, it has not been widely tied to specific mineralogical examples.

For these reasons and also because of a growing emphasis on synchrotron studies to address problems of oxidation state and site occupancy of Fe in minerals (e.g., Henderson et al. 1995) that also need the interpretation of the electronic structure of Fe in various sites, we are motivated to present spectroscopic data for a series of tetrahedral Fe^{2+} standards (gehlenite, genthelvite, pellyite, spinel, and staurolite) as well as two minerals, grandidierite and joaquinite, that provide site distortions and coordination environments intermediate between tetrahedral and octahedral.

EXPERIMENTAL DETAILS

Sample preparation

The samples for investigation were prepared as parallel plates, polished on both sides. The final thickness of each sample depends mainly on the concentration of Fe^{2+}. The samples were thinned until the maximum absorbance of spin-allowed Fe^{2+} bands did not exceed 1.7.

* E-mail: grr@gps.caltech.edu

[1]Permanent address: Institute of Geochemistry, Mineralogy and Ore Formation, National Academy of Science of Ukraine, pr. Palladina 34, 03142 Kyiv, Ukraine

For all minerals except pellyite and gillespite, the samples were prepared as self-supporting plates. The latter two minerals have a perfect cleavage perpendicular to the *c*-axis. In addition, pellyite was available as small (~1 mm) grains of low strength and, therefore, could only be ground and polished after fixing in an embedding material. Therefore, both pellyite and gillespite samples have been prepared as thin sections, fixed to supporting glass plates with epoxy resin. Table 1 presents information on localities, FeO content and color of the samples. Their orientation and thickness are compiled in Table 2.

Optical and IR spectroscopy

Polarized optical absorption spectra in the 350–1700 nm range were obtained at about 1 nm resolution with a home-built microspectrometer system consisting of a 1024 element Si- and a 256 element InGaAs diode-array detector coupled to a grating spectrometer system attached via fiber optics to a highly modified NicPlan infrared microscope containing a calcite polarizer. In the range 10 000–2500 cm^{-1} polarized spectra were measured with Magna-IR 860 FTIR spectrometer using an InSb detector, CaF_2 beamsplitter, SiC source and a $LiIO_3$ crystal polarizer. The spectral resolution was 4 cm^{-1}. The measurement area was defined by an aperture whose size varied, depending on dimension and quality of the samples, from 25–200 μm. Between 64 and 500 scans were collected for each spectrum.

To evaluate energy, peak intensity and half-width of the Fe^{2+} spin-allowed bands, Peakfit 4.0 (Jandel Scientific) software was used to fit the spectra after they were first converted to a linear wavenumber scale. Of all functions available, the Gaussian forms were found to best fit the spectra. The number of components used in the fits was always chosen to seem reasonable from visual inspection of the spectra. Although for some minerals differently polarized components derived by curve resolution differ in energies and half-widths (Table 2), they may be regarded as polarized components of one band. This is probably true for the gehlenite bands around 5000 and 6300 cm^{-1}, the grandidierite band at 10 000 cm^{-1} and the bands in the range of 11 000–12 000 cm^{-1} in the joaquinite spectrum. Differences in the band positions (ν) and halfwidths ($\nu_{1/2}$) of such components may originate, at least partly, from the fitting procedure.

Sample compositions

Compositions of minerals were generally available from the literature as referenced in Table 1. In the case of gehlenite, gillespite, joaquinite, and spinel, the spectra were obtained from the exact samples on which the analyses were obtained. Other compositions are representative of the locality from which the samples come. In the case of grandidierite, a new analysis was obtained on a JEOL 733 electron microprobe. The Fe content is reported in Table 1.

TABLE 2. Spectroscopic properties of Fe^{2+}

Mineral	Polarization	Thickness μm	Energy, ν, (cm^{-1}); half-width, $\nu_{1/2}$, (cm^{-1}); and molar absorption coefficient, ε, (cm^{-1} l mol^{-1}) of the bands
eudialyte	**E⊥c**	373	(18900, 2750, 4.7), (7320, 1130, 0.9)
	E‖c	373	(18760, 2660, 4.7)
gehlenite	**E⊥c**	164	(6340, 2580, 33), (5050, 1750, 1)
	E‖c	164	(6200, 2210, 11); (4970, 1430, 11)
genthelvite	–	41	(4990, 1280, 30), (4140, 1370, 44), (3410, 240, 3), (3030, 440, 20)
gillespite	**E⊥c**	100	(20260, 3300, 1.7), (8380, 1610, 0.6)
	E‖c	100	(19600, 3360, 10.8)
grandidierite	α	579	(13040, 5100, 25), (10530, 2000, 9.4), (5020, 1380, 21)
	β	579	(9730, 1630, 6)
	γ	760	(12540, 4630, 11), (10100, 1870, 6)
joaquinite	α	31	(9590, 2612, 48), (12550, 2420, 7)
	β	24	(~11000, ~2600, 5), (4780, 1300, 12)
	γ	24	(~10900, ~3000, 10), (4500, 1420, 13)
pellyite	α	28	(7390, 1480, 91), (5820, 700, 34)
	β	28	–
	γ	32	(7020, 1090, 42), (5850, 750, 45), (5250, 200, 9)
spinel	–	503	(5370, 1480, 31), (4710, 1260, 53), (4060, 300, 7), (3680, 630, 42)
staurolite	α	62	(5490, –, 39)
	β	64	(3900, –, 39)
	γ	62	(5370, –, 35)

RESULTS

In the spectra of all minerals studied (Figs. 1–3, and others later in text), broad, intense absorption bands caused by electronic, spin-allowed *dd* transitions of Fe^{2+} ($^5E \rightarrow {}^5T_2$ transition in T_d-symmetry) are the dominant spectroscopic features. The information on energy, half-width and molar absorption coefficients of the spin-allowed bands, obtained from curve fitting, is gathered in Table 2. Low intensity (ca. two orders weaker than the $^5E \rightarrow {}^5T_2$ bands of Fe^{2+}) bands, caused by Fe^{2+} spin-forbidden transitions and by low concentrations of some other transition metal ions such as Cr^{3+} in spinel or Mn^{2+} in genthelvite (Fig. 2) appear in the visible range. In the staurolite spectrum

TABLE 1. Sample descriptions and analyses

Sample number	Mineral	Locality	Color	wt% FeO	Source of analysis
GRR 160	eudialyte	Kukiscumchorr deposit, Kola Peninsula, Russia	crimson-red	4.67	Pol'schin et al. (1991)
CIT 8013	gehlenite	Christmas Mountains, Texas, U.S.A.	pale amber	4.04	Joesten (1974)
CIT 9305	genthelvite	Diamond Hill, Rhode Island, U.S.A.	rose	10.79	Hassan and Grundy (1985)
CIT 1768	gillespite	Incline, Maraposa County, California, U.S.A.	red	25.26	Gaffney (1973)
CIT 8376	grandidierite	Metroka, Madagascar	greenish-blue	1.10	our analysis
GRR 158	joaquinite	Gem Mine, San Benito County, California, U.S.A.	pale amber	3.4	Rossman (1975)
GRR 334	pellyite	Ross River, Yukon Territory, Canada	pale amber	12.18	Pabst and Harris (1984)
RDS-153	spinel*	gem gravel, Tanzania	pink	1.03	Sp3 of Shannon & Rossman (1991)
CIT 7520	staurolite	Pizzo Forno, Leventina, Switzerland	brownish-yellow	12.22	Hawthorne et al. (1993)

* *Note:* additional spinels used for Figures 1 and 2: Samples Sp1 (0.40 wt% FeO), Sp2 (1.00 wt% FeO), Sp4 (0.08 wt% FeO), Sp5 (0.28 wt% FeO), and Sp6 (0.00 wt% FeO) of Shannon and Rossman (1991), where total iron is expressed as wt% FeO.

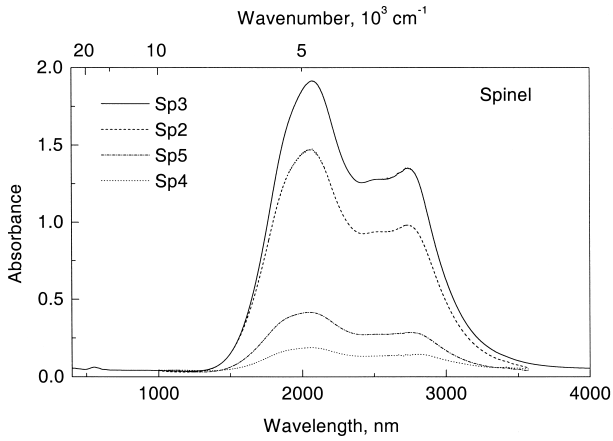

FIGURE 1. Optical absorption spectra of spinels plotted for 0.50 mm thick samples. Sample numbers from bottom to top: Sp4, Sp5, Sp2, Sp3.

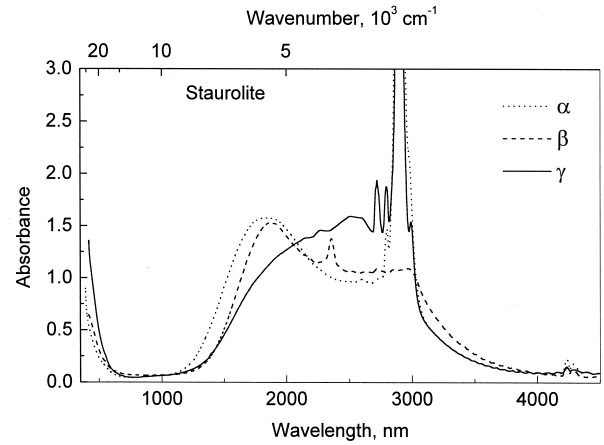

FIGURE 3. Polarized optical absorption spectra of staurolite from Pizzo Forno, Switzerland, plotted for a sample thickness of 0.060 mm.

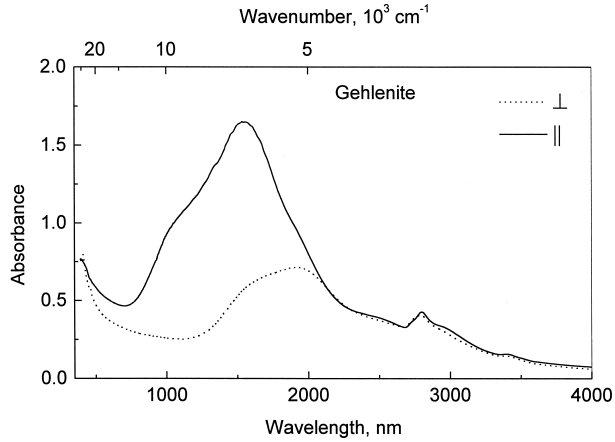

FIGURE 2. Polarized optical absorption spectra of gehlenite from the Christmas Mountains, Texas, plotted for a sample thickness of 0.20 mm.

(Fig. 3) the short-wave absorption edge is likely caused by Fe^{3+} ions ($O^{2-} \rightarrow Fe^{3+}$ charge transfer transitions).

In some minerals the near-infrared Fe^{2+} bands are partly overlapped by narrow, intense OH absorption bands that present additional difficulties for curve fitting analysis. In the case of the staurolite spectra the OH-bands in the 2900 nm range (3450 cm^{-1}) are so strong (Fig. 3) that energies and peak intensities of the Fe^{2+} bands could only be estimated from visual observation (Table 2), and the halfwidth could not be reliably estimated at all. Complete spectroscopic data files are available at http://minerals.gps.caltech.edu/manuscripts/Tetrahedral_Standards/Index.html.

Spinel

In spinel, $MgAl_2O_4$, small amounts of $^{IV}Fe^{2+}$ give rise to a group of bands in the near-infrared region. The Mössbauer study of Dickson and Smith (1976) as well as several optical spectroscopic studies have shown that in low-Fe spinel, Fe occupies the T site. X-ray structure refinements of $MgAl_2O_4$ (e.g., Yamanaka and Takéuchi 1983) indicate that the T site is a regular tetrahedral site with T_d point symmetry. A perfect tetrahedral site ideally would give rise only a single absorption band, caused by the $^5E \rightarrow {}^5T_2$ transition in $^{IV}Fe^{2+}$.

The spectra of spinels contain more detail than the one band expected from crystal field theory. The spectra of a series of spinels with low concentrations of Fe are presented in Figure 1. Four components can be visually identified in the main band complex. One of these components is at about 2720 nm (3680 cm^{-1}), an energy at which trace OH commonly appears in mineral spectra. The constant intensity ratio of all the bands (that extends to spinels with an nearly an order of magnitude more Fe than those illustrated in Fig. 1) indicates that all of these bands come from Fe and none come from OH.

The observed splitting (Fig. 1, Tables 2 and 3) could be a result of the dynamic Jahn-Teller effect, which changes the symmetry of vibronic states of the FeO_4^{6-} complex and thus splits the $^5E \rightarrow {}^5T_2$ band. The Jahn-Teller effect should be especially strong in a case when the ground electronic state is a doubly degenerate *E*-state (Bersuker 1996). Another possible contribution to the splitting could be next-nearest interactions brought about by local clustering of the Fe^{2+}.

The spectrum of spinel RDS-153 was fitted with both two- and four-band models. The parameters listed in Table 2 are for the four-band model. The choice of model has only a modest effect on the correlation presented in the discussion section. Spinel displays the smallest splitting of the $^5E \rightarrow {}^5T_2$ band among all minerals studied, which is consistent with the regular character of the tetrahedral site in its structure.

The correlation of intensity of the band maximum at approximately 2100 nm with total Fe (as FeO wt%) is presented in Figure 4. The deviations from a linear trend are most likely due to overrepresentation of the actual FeO content due to a Fe^{3+} component in some of the crystals.

Pellyite

In the spectrum of pellyite, $Ba_2Ca(Fe,Mg)_2Si_6O_{17}$, (Fig. 5) three distinct bands occur in the range of the $^5E \rightarrow {}^5T_2$ transition of $^{IV}Fe^{2+}$ (Table 2). The feature around 2500 nm in γ-polar-

ization is caused by absorption by the imbedding epoxy resin. Bands around 5850 cm^{-1} (1710 nm) differ in energies and half-widths (Table 2). They may be regarded as polarized components of one band. These differences in position (ν) and band width ($\nu_{1/2}$) may originate, at least partly, from the fitting procedure.

The results of the fitting procedure show that a shoulder around 5250 cm^{-1} (1905 nm) in γ-polarization is narrow ($\nu_{1/2}$ ~200 cm^{-1}) compared to the other three bands. Although it is in a region where combination mode vibrations of water molecules occur, the absence of a water fundamental vibration in the 3500 cm^{-1} region indicates that this band is not from this cause. In spite of the unusually small width, it is assigned to a $^{IV}Fe^{2+}$ *dd* transition. The splitting of the $^5E \rightarrow {}^5T_2$ transition to three components means that the degeneracy of the excited $^5T_2$–state is completely lifted due to low symmetry of the Fe^{2+}-bearing tetrahedral site. The latter, in contrast to the spinel site, is distorted in terms of both the bond-length (BLDP) and edge-length distortion parameters (ELDP) (Table 3).

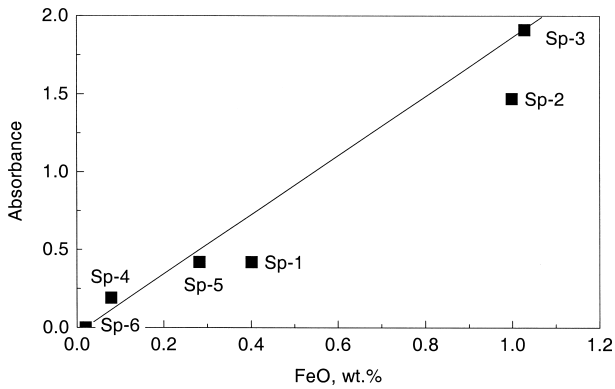

FIGURE 4. Correlation of the intensity of the band at 4760 cm^{-1} (2100 nm) with the total Fe content (expressed as wt% FeO) for $MgAl_2O_4$ spinels that contain small amounts of Fe.

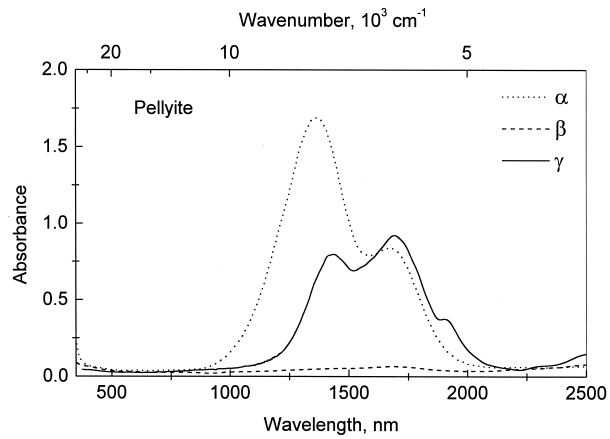

FIGURE 5. Polarized optical absorption spectra of pellyite from Yukon Territory, Canada, plotted for a sample thickness of 0.030 mm.

Gehlenite

Gehlenite is a member of the melilite group with an ideal formula $Ca_2Al(AlSi)O_7$. Fe^{2+} substitutes for Al in a tetrahedral site. In the spectrum of gehlenite (Fig. 2), there are multiple bands. Two bands with maxima around 4970 cm^{-1} (2012 nm, **E**⊥**c**) and 6250 cm^{-1} (1600 nm, **E**∥**c** > **E**⊥**c**) are readily assigned to components of the $^5E \rightarrow {}^5T_2$ transition of $^{IV}Fe^{2+}$.

A band near 9220 cm^{-1} (1085 nm, **E**∥**c**), seen in the spectrum as a shoulder on the high-energy side of the 1600 nm band is at too high an energy to be attributed to *dd*-transitions of tetrahedral Fe^{2+} and at too low an energy to be caused by Fe^{2+}/Fe^{3+} intervalence charge transfer transition (e.g., Burns 1993). Another cation site in the gehlenite structure that can accommodate some amount of Fe^{2+} is the Ca-bearing polyhedron (Smith 1953). It is quite possible that the shoulder is caused by spin-allowed *dd* transitions in $^{Ca}Fe^{2+}$.

The bands at about 2800 – 3000 nm (3570–3330 cm^{-1}) are problematic. The full width at half height of the 2800 nm band is ~150 cm^{-1}, a value too narrow for most spin-allowed *dd* bands. This band is in a region appropriate for OH and normally it would be assigned to minor amounts of OH in the sample. The narrowness of the pellyite band at ~1900 nm that can only be assigned to Fe^{2+} complicates the assignment of the 2800 nm band in gehlenite to OH. No other samples of melilites with different Fe concentrations were available for this study, so rigorous proof of an OH or Fe origin is lacking at this time. For purposes of the tables, this band is not considered to originate from Fe^{2+}.

The splitting of the $^5T_2$ level of $^{IV}Fe^{2+}$ into two components, 4970 cm^{-1} (**E**⊥**c**) and 6250 cm^{-1} (**E**∥**c** > **E**⊥**c**), is consistent with a comparatively high symmetry of the tetrahedral site that keeps all Fe-O distances equal (BLDP = 0). A low ELDP-value (Table 3) is evidence for only a slight bond angle distortion of the position.

Staurolite

In the spectrum of staurolite, $Fe_4Al_{18}Si_8O_{46}(OH)_2$ (Fig. 3), one can identify two bands that are undoubtedly caused by spin-allowed transitions in $^{IV}Fe^{2+}$: ~3900 cm^{-1} (2560 nm) (γ) and 5400 cm^{-1} (1850 nm) ($\alpha \approx \beta > \gamma$). Mössbauer studies (Dowty 1971) confirm that most of the Fe resides in the tetrahedral site. In staurolite from Pizzo Forno, studied by Dyar et al. (1991), 80% of total Fe content enters tetrahedral sites as Fe^{2+} and only 10% of the total amount occupies the octahedral sites as Fe^{2+}. Although the geometric distortion of the tetrahedral site in the staurolite structure is comparatively low (Table 3), the presence of two types of differently charged ligands, O^{2-} and OH^-, in the coordination tetrahedron, causes the $^5T_2$ level to split into two well-separated components (Tables 2 and 3).

Genthelvite

Genthelvite, $Zn_8(Be_6Si_6O_{24})S_2$, forms a solid solution series toward danalite, $Fe_8(Be_6Si_6O_{24})S_2$. In these minerals, Fe^{2+} occupies a tetrahedral site bonded to three O atoms and one S (Hassan and Grundy 1985). In the spectrum of genthelvite, the $^5E \rightarrow {}^5T_2$ band of $^{IV}Fe^{2+}$ is split into three distinct bands that are best fit by a four band fit with components at 4990, 4140, 3410, and 3030 cm^{-1} (Fig. 6, Table 2).

TABLE 3. Crystal chemical formula, space group symmetry, coordination surrounding, dimension, distortion of Fe^{2+} sites and splitting of spin-allowed bands

Mineral	Ideal chemical formula	Fe^{2+} site	Fe^{2+} coordination	$(Fe\text{-}Ligand)_{av}$, Å	(BLDP)*	(ELDP)*	(BLDP) + (ELDP)	Barycenter energy cm^{-1}	Band splitting cm^{-1}
eudialyte	$Na_{12}Ca_7Fe_3Zr_3Si[Si_3O_9]_2[Si_9O_{27}]_2(OH)_2Cl_2$	M(2,4)†	$4O^{2-}$	2.1000	0	0.1896	0.1896	13000	11550
gehlenite	$Ca_2(Al,Fe,Mg)(Si,Al)_2O_7$	(Mg, Al)‡	$4O^{2-}$	1.8832	0	0.0087	0.087	5820	1330
genthelvite	$Zn_8(Be_6Si_6O_{24})S_2$	C-site§	$3O^{2-} + S^{2-}$	2.0615	0.0909	0.0675	0.1584	3890	1960
gillespite	$BaFeSi_4O_{10}$	FeII	$4O^{2-}$	1.9666	0	0.1535	0.1535	13900	11297
grandidierite	$(Mg,Fe)Al_3BSiO_9$	Mg#	$5O^{2-}$	2.0403	–	–	–	8840	7200
joaquinite	$Ba_4Fe_2RE_4Ti_4O_4[Si_4O_{12}](OH)_2$	Fe**	$4O^{2-}OH^-$	2.1064	–	–	–	8890	8050
pellyite	$Ba_2Ca(Fe,Mg)_2Si_6O_{17}$	Fe††	$4O^{2-}$	2.0091	0.0348	0.0999	0.1347	6160	2140
spinel	$MgAl_2O_4$	T‡‡	$4O^{2-}$	1.9173	0	0	0	4460	1690
staurolite	$Fe_4Al_{18}Si_8O_{46}(OH)_2$	T(2)§§	$2O^{2-}+2OH^-$	2.0037	0.0187	0.0105	0.0337	4700	1520

* Tetrahedral bond-length distortion parameter, BLDP; Tetrahedral edge-length distortion parameter, ELDP, Griffen and Ribbe (1979).
† Johnsen and Grice (1999).
‡ Smith (1953); Seifert et al. (1987).
§ Hassan and Grundy (1985), Maeda et al. (1985), Nimis et al. (1996).
|| Pabst (1943).
Stephenson and Moore (1968).
** Dowty (1975)0.
†† Meagher (1976).
‡‡ Yamanaka and Takéuchi (1983); Carbonin et al. (1996).
§§ Tagai and Joswig (1985); Hawthorne et al. (1993).

The comparatively strong splitting of the bands (Tables 2 and 3) is likely due to the presence of an S^{2-} anion in the coordination sphere. The S anion is more remote from the central atom than the three O atoms (2.343 Å and 1.968 Å, respectively) and thus results in a comparatively strong distortion of the FeO_4S-tetrahedron (Table 3).

Gillespite and eudialyte

Spectra of gillespite, $BaFeSi_4O_{10}$, (Fig. 7) and eudialyte, $Na_{12}Ca_7Fe_3Zr_3Si[Si_3O_9]_2[Si_9O_{27}]_2(OH)_2Cl_2$, (Fig. 8) are similar. This reflects the square-planar O coordination of Fe^{2+} in both minerals. The electronic level scheme of Fe^{2+} ion in such coordination significantly differs from Fe^{2+} in tetrahedral sites (Burns et al. 1966; Bersuker 1996; Marfunin 1979). As a result, some of the bands in the spectra of gillespite and eudialyte that originate from spin-allowed Fe^{2+} transitions are shifted to much higher energies.

In both minerals Fe^{2+} causes spectacular color and, in gillespite, strong pleochroism. Due to the centrosymmetric character of the Fe^{2+} sites, the bands are comparatively weak (Table 2). They are formally forbidden by the Laporte selection rule, and become allowed only due to odd thermal vibrations of the surrounding ligands (Burns et al. 1966; Pol'shin et al. 1991). In eudialyte this causes a distinct dependence of intensity on temperature (Pol'shin et al. 1991).

Grandidierite

The spectrum of grandidierite, $(Mg,Fe)Al_3BSiO_9$, (Fig. 9) resembles the spectra of minerals with Fe^{2+} in strongly distorted octahedral coordination, such as Fe^{2+}(M2) in orthopyroxenes (Goldman and Rossman 1977a) or Fe^{2+}(M4) in calcic amphiboles (Goldman and Rossman 1977b). All of these have a large energy difference between the high- and low-energy bands, and show a large difference in the intensity of the components. In contrast to the spectra of amphiboles and pyroxenes that usually display two bands originating from electronic transition to the split ^5E_g-level, in the grandidierite spectrum one can distinguish four bands that may be attributed to spin-allowed transitions in Fe^{2+} (Table 2). This could occur because Fe^{2+} occupies

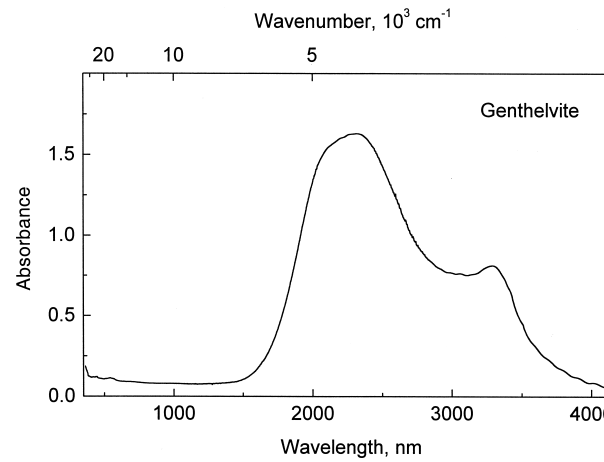

FIGURE 6. Optical absorption spectra of genthelvite from Diamond Hill, Rhode Island, U.S.A., plotted for a sample thickness of 0.040 mm. The weak oscillations near 4000 nm are interference fringes from the thin sample.

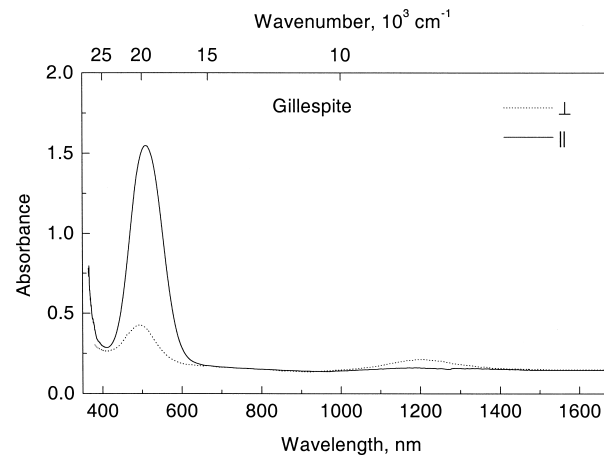

FIGURE 7. Polarized optical absorption spectra of gillespite from Incline, California, plotted for a sample thickness of 0.10 mm.

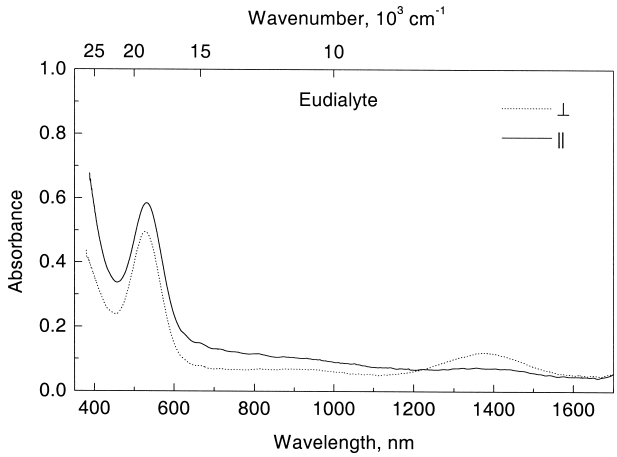

FIGURE 8. Polarized optical absorption spectra of eudialyte from the Kola Peninsula, Russia, plotted for a sample thickness of 0.40 mm.

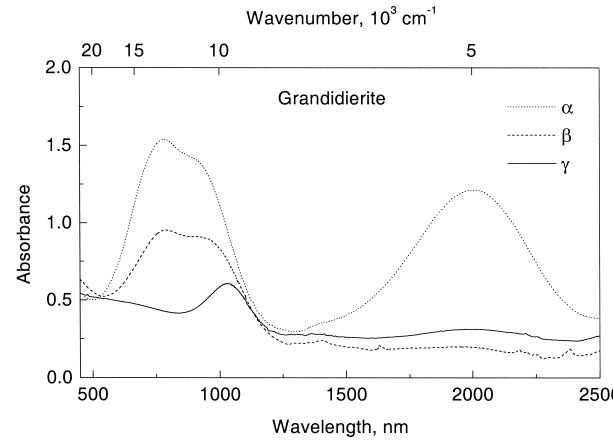

FIGURE 9. Polarized optical absorption spectra of grandidierite from Metroka, Madagascar, plotted for a sample thickness of 1.00 mm.

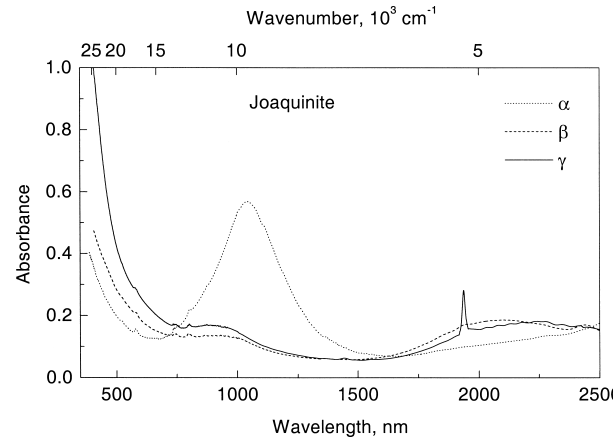

FIGURE 10. Polarized optical absorption spectra of joaquinite from the Gem Mine, San Benito County, California, plotted for a sample thickness of 0.050 mm.

multiple, non-equivalent sites or because the energy level scheme of $^{V}Fe^{2+}$ is so different from that of $^{IV}Fe^{2+}$ that all four transitions between levels of the split ^5D-term of Fe^{2+} appear in the near infrared (NIR) range. Investigations of the Mössbauer spectroscopy of grandidierite concluded that Fe^{2+} is sited mostly in the MgO_5 trigonal bipyramid (Seifert and Olesch 1977; Qiu et al. 1990). Therefore, it is probable that all four absorption bands observed in optical spectra of grandidierite (Fig. 9) are caused by spin-allowed electronic transitions of $^{V}Fe^{2+}$.

Joaquinite

In the optical spectrum of joaquinite, $Ba_4Fe_2RE_4Ti_4O_4[Si_4O_{12}](OH)_2$, (Fig. 10) three absorption bands may be considered spin-allowed *dd*-transitions of $^{V}Fe^{2+}$ (Table 2) assuming that the bands at ~11000 cm^{-1} ($\beta \approx \gamma$) and ~12550 cm^{-1} (α) are polarized components of the same electronic transition. As in the case of grandidierite discussed above, the number of bands assigned to spin-allowed *dd* transitions of Fe^{2+} is consistent with non-octahedral, fivefold coordination of Fe^{2+} ions in the joaquinite structure. A number of sharp bands appear throughout the spectrum from rare earth and H_2O absorption. A more detailed discussion of the joaquinite spectrum is presented in Rossman (1975).

DISCUSSION

Information on average metal-ligand distances in coordination polyhedra, distortion of Fe^{2+} sites in terms of bond-length and edge-length distortion parameters (Griffen and Ribbe 1979) derived from X-ray structural refinement data, barycenter energy and splitting of the $^5E \rightarrow {}^5T_2$ transition, calculated from optical absorption spectra in Figures 1–3 and 5–10, is compiled in Table 3.

Band intensity

The molar absorption coefficients (ε) of the more intense spin-allowed bands of tetrahedral Fe^{2+} ions range from ~20 cm^{-1}·L·mol^{-1} to ~90 cm^{-1}·L·mol^{-1} (Table 2). These values are much higher than those of Fe^{2+} in weakly distorted octahedral sites and commensurate with Fe^{2+} in strongly distorted sites such as the M2 position in orthopyroxene (41 cm^{-1}·L·mol^{-1}) or M4 in calcic amphibole (>27 cm^{-1}·L·mol^{-1}) (e.g., Goldman and Rossman 1977b; Burns 1993). The bands caused by Fe^{2+} in square-planar O coordination in the gillespite and eudialyte spectra are much weaker, consistent with the centrosymmetry of the sites.

Band polarization

In the optically anisotropic minerals, bands caused by spin-allowed transitions of Fe^{2+} in fourfold coordination display distinct polarization dependencies. The spectrum of pellyite (Fig. 5), which contains strong bands in α- and γ-polarizations but almost none in the β-spectrum, is the most distinctive example. Such polarization behavior indicates that the individual electronic transitions of $^{IV}Fe^{2+}$ are subject to selection rules as a result of the lowered symmetry of the sites. For pellyite, where the anisotropic properties of the bands are most spectacular, the degree of distortion of the site in terms of BLDP+ ELDP is

the largest among anisotropic minerals with tetrahedral Fe^{2+} coordination (Table 3).

The group theory approach to the polarization properties is, however, more transparent in the case of the octahedral coordination compared to the tetrahedral one. In the case of octahedral coordination, the distorted sites are modeled by allowing them to descend from O_h to lower symmetries. According to this model, all transitions are forbidden in a regular octahedron whereas some of them become allowed in distorted octahedral sites due to the absence of symmetry elements such as a center of symmetry (e.g., Bersuker 1996). In the case of tetrahedral coordination the opposite situation exists. In a regular tetrahedron all transitions are symmetry-allowed, but in sites of symmetry lower than T_d, some of the transitions may be forbidden for certain orientations of the incident electric vector.

Furthermore, when the distortions from tetrahedral symmetry are great, some new elements of symmetry that are different from those of the T_d-group may appear, which also influence the selection rules. The square-planar coordination may be regarded as an extreme example of such distortion leading to a number of new symmetry elements, including a center of symmetry, that cause all transitions of $^{IV}Fe^{2+}$ to be forbidden. In practice some transitions may become allowed due to the vibrations of the surrounding ligands that cause dynamic deviation from centrosymmetry. Such a situation takes place in gillespite and eudialyte, minerals with centrosymmetric square-planar Fe^{2+} coordination, where the electronic transitions are allowed due to this coupling with the vibrations of the surrounding ligands, and are strictly polarized along particular crystallographic directions (Burns et al. 1966; Pol'shin et al. 1991).

Other spectroscopic parameters

As is seen from Table 3, the values of the barycenter and splitting of the spin-allowed bands of Fe^{2+} for minerals with Fe^{2+} in tetrahedral coordination (gehlenite, genthelvite, pellyite, spinel, and staurolite) group separately from those minerals in which Fe^{2+} has square-planar (eudialyte and gillespite) or pyramidal fivefold coordination (grandidierite and joaquinite).

For the four minerals with a purely O tetrahedral environment around Fe^{2+} (gehlenite, pellyite, spinel and staurolite) there is a correspondence between the distortion of the tetrahedral environment, (BLDP) + (ELDP), and the energy of the barycenter of the spin-allowed bands (Fig. 11). This dependence is, most probably, due to splitting of the electronic ground state. As Figure 12 shows, the barycenter energy should increase approximately by the value $\delta/2$, the splitting of the electronic ground state, caused by distortion of the site. It should be noted that in the case of distorted octahedral coordination the contribution of the splitting of the ground level to the energies and barycenter of spin-allowed *dd* bands of $^{VI}Fe^{2+}$ should be much less than in tetrahedral coordination and, therefore, a correlation like that in Figure 11 would hardly maintain for $^{VI}Fe^{2+}$. Indeed, in the case of $^{VI}Fe^{2+}$ the energy of spin-allowed transition $^5T_{2g} \rightarrow {}^5E_g$ is greater than that of $^5E \rightarrow {}^5T_2$ in $^{IV}Fe^{2+}$ and hence a relative contribution due to splitting of the ground $^5T_{2g}$ level (analogous of $\delta/2$, Fig. 12) should be lower. Also, in octahedral coordination the splitting of the triply degenerate $^5T_{2g}$ level may be smaller than that of the doubly degenerate ^5E level in $^{IV}Fe^{2+}$. To our knowledge, in the literature there is no evidence of a correlation between barycenter energy of spin-allowed *dd* bands of $^{VI}Fe^{2+}$ and distortion of an octahedral site.

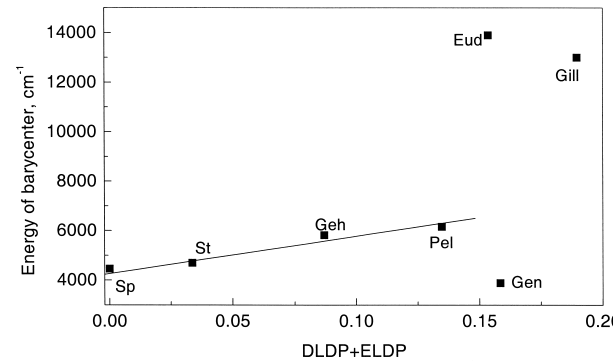

FIGURE 11. Plot of the barycenter energy of the spin-allowed Fe^{2+} *dd* bands vs. the sum of the bond length (BLDP) and edge length (ELDP) distortion parameters for minerals with Fe in four coordination.

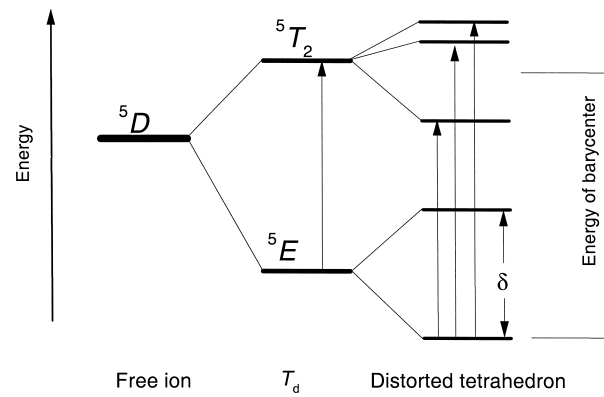

FIGURE 12. Splitting of the ^5D electronic term in regular (T_d) and distorted tetrahedral sites. Arrows show possible electronic transitions. The barycenter energy increases by approximately the value $\delta/2$ in a distorted site.

The barycenter energy is not correlated with either BLDP or ELDP, individually, in the studied minerals. In the case of genthelvite, where the ligands surrounding $^{IV}Fe^{2+}$ are O_3S, the situation is perturbed by the S and the correlation is not maintained. The correlation also is not maintained when the coordination is square planar (gillespite and eudialyte). Systems with Fe in fivefold coordination (grandidierite and joaquinite) do not follow the trend for tetrahedral Fe^{2+}.

The results of this study also point to the need for more extensive theoretical analysis of the spectra of Fe^{2+} in tetrahedral sites. Questions remain about the detailed assignment of the bands in general and about the origin of the unusually narrow bands in particular.

ACKNOWLEDGMENTS

Support for this project was provided by National Science Foundation (U.S.A.) grant EAR-9804871 as part of the program for eastern European collaboration. We thank Ray Joesten for providing the analyzed gehlenite sample, Buzz Gray for the joaquinite, and Pat Meagher and Lee Groat for providing the pellyite samples.

REFERENCES CITED

Bersuker, I.B. (1996) Electronic structure and properties of transition metal compounds: introduction to the theory. Wiley, New York.

Burns, R.G. (1993) Mineralogical applications of crystal field theory. Cambridge University Press, Cambridge.

Burns, R.G., Clark, M.G., and Stone, A.J. (1966) Vibronic polarization in the electronic spectra of gillespite, a mineral containing iron(II) in square-planar coordination. Inorganic Chemistry, 5, 1268–1272.

Carbonin, S., Russo, U., and Della Guiusta, A. (1996) Cation distribution in some natural spinels from X-ray diffraction and Mössbauer spectroscopy. Mineralogical Magazine, 60, 355–368.

Dickson, B.L. and Smith, G. (1976) Low-temperature optical absorption and Mössbauer spectra of staurolite and spinel. Canadian Mineralogist, 14, 206–215.

Dowty, E. (1971) Site distribution of iron in staurolite. Earth and Planetary Sciences Letters, 15, 72–74.

Dowty, E. (1975) Crystal structure of joaquinite. American Mineralogist, 60, 872–878.

Dyar, M.D., Perry, C.L., Rebbert, C.R., Dutrow, B.L., Holdaway, M.J., and Lang, H.M. (1991) Mössbauer spectroscopy of synthetic and naturally occurring staurolite. American Mineralogist, 76, 27–41.

Gaffney, E. (1973) Crystal field effects in mantle minerals, 216 p. Thesis, California Institute of Technology, Pasadena, CA,

Goldman, D.S. and Rossman, G.R. (1977a) The spectra of iron in orthopyroxene revisited: the splitting of the $^5T_{2g}$ ground state. American Mineralogist, 62, 151–157.

———(1977b) The identification of Fe^{2+} in the M(4) site of calcic amphiboles. American Mineralogist, 62, 205–216.

Goldman, D.S., Rossman, G.R., and Parkin, K.M. (1978) Channel constituents in beryl. Physic and Chemistry of Minerals, 3, 225–235.

Griffen, D.T. and Ribbe, P.H. (1979) Distortions in the tetrahedral oxyanions of crystalline substances. Neues Jahrbuch für Mineralogie. Abhandlungen, 137, 54–73.

Hassan, I. and Grundy, H.D. (1985) The crystal structure of helvite group minerals, $(Mn,Fe,Zn)_8(Be_6Si_6O_{24})S_2$. American Mineralogist, 70, 186–192.

Hawthorne, F.C., Ungaretti, L., Oberti, R., Caucia, F., and Callegari, A. (1993) The crystal chemistry of staurolite: I. Crystal structure and site populations. Canadian Mineralogist, 31, 532–551.

Henderson, C.M.B., Cressey, G., and Redfern, S.A.T. (1995) Geological applications of synchrotron radiation. Radiation Physics and Chemistry, 45, 459–81.

Joesten, R. (1974) Pseudomorphic replacement of melilites by idocrase in a zoned calc silicate skarn, Christmas Mountains, Big Bend Region, Texas. American Mineralogist, 59, 694–699.

Johnsen, O. and Grice, J.D. (1999) The crystal chemistry of the eudialyte group. Canadian Mineralogist, 37, 865–891.

Marfunin, A.S. (1979) Physics of minerals and inorganic materials: an introduction. Springer-Verlag, New York.

Maeda, Y., Takashima, Y., and Ishida, K. (1985) Mössbauer spectroscopic study of danalite, $Fe_4(BeSio_4)_3S$. Bulletin of the Chemical Society of Japan, 58, 1047–1048.

Meagher, E.P. (1976) The atomic arrangement of pellyite; $Ba_2Ca(Fe,Mg)_2Si_6O_{17}$. American Mineralogist, 61, 67–73.

Nimis, P., Molin, G., and Visona, D. (1996) Crystal chemistry of danalite from Daba Shabeli Complex (N Somalia). Mineralogical Magazine, 60, 375–379.

Pabst, A. (1943) Crystal structure of gillespite, BaFeSi4O40 (Alaska, California). American Mineralogist, 28, 372–390.

Pabst, A. and Harris, J. (1984) Pellyite: new localities and new data. Canadian Mineralogist, 22, 653–658.

Platonov, A.N., Taran, M.N., Pol'shin, E.V., and Min'ko, O.Y. (1979) On the nature of colour of iron-bearing beryls. Izvestiya Akademii Nauk SSSR. Seriya Geologicheskaya, 54–68 (in Russian).

Pol'shin, E.V., Platonov, A.N., Borutzky, B.E., Taran M.N., and Rastsvetaeva, R.K. (1991) Optical and Mössbauer study of minerals of the eudialyte group. Physics and Chemistry of Minerals, 18, 117–125.

Price, D.C., Vance, E.R., Smith, G., Edgar, A., and Dickson, B.L. (1976) Mössbauer effect studies of beryl. Journal de Physique. Colloques, 37, C6.811–C6.817.

Qiu, Z., Rang, M., and Chang, J. (1990) Mössbauer spectra of grandidierite**.** Chinese Science Bulletin, 35, 43–7.

Rossman, G.R. (1975) Joaquinite: the nature of its water content and the question of four-coordinated ferrous iron. American Mineralogist, 60, 435–440.

Seifert, F. and Olesch, M. (1977) Mössbauer spectroscopy of grandidierite, $(Mg,Fe)Al_3BSiO_9$. American Mineralogist, 62, 547–553.

Seifert, F., Czank, M., Simons, B., and Schmahl, W. (1987) A commensurate incommensurate phase transition in iron bearing melilites. Physics and Chemistry of Minerals, 14, 26–35.

Shannon, R.D. and Rossman, G.R. (1991) Dielectric constant of $MgAl_2O_4$ spinel and the oxide additivity rule. Journal of the Physics and Chemistry of Solids, 52, 1055–1059.

Slack, G.A. (1964) $FeAl_2O_4$-$MgAl_2O_4$: growth and some thermal, optical and magnetic properties of mixed single crystals. Physical Review, 134A, 1268–1280.

Smith, J.V. (1953) Reexamination of the crystal structure of melilite. American Mineralogist, 38, 643–661

Stephenson, D.A. and Moore, P.B. (1968) The crystal structure of grandidierite, $(Mg, Fe)Al_3SiBO_9$. Acta Crystallographica, 24B, 1518–1522.

Tagai, T. and Joswig, W. (1985) Untersuchungen der Kationenverteilung im Staurolith durch Neutronenbeugung bei 100 K. Neues Jahrbuch für Mineralogie. Monatshefte, 3, 97–107.

Taran, M.N., Klyakhin, V.A., Platonov, A.N., Pol'shin, E.V., and Indutny, V.V. (1989) Optical spectra of natural and artificial iron-containing beryls at 77–297 K. Soviet Physics. Crystallography, 34, 882–884.

Yamanaka, T. and Takéuchi, Y. (1983) Order-disorder transition in $MgAl_2O_4$ spinel at high temperatures up to 1700 °C. Zeitschrift für Kristallographie, 165, 65–78.

MANUSCRIPT RECEIVED SEPTEMBER 11, 2000
MANUSCRIPT ACCEPTED MARCH 29, 2001
PAPER HANDLED BY CELIA MERZBACHER